Error Analyses and Modeling for CEBAF Beam Optical Systems: Beam Line Element Specifications and Alignment Error Tolerances*

D.R. Douglas, J.Y. Tang, and R.C. York†

Continuous Electron Beam Accelerator Facility
12000 Jefferson Avenue
Newport News, VA. 23606

ABSTRACT

A description of error analyses and computer modeling of the CEBAF transport system is given. The impact of various perturbations, including magnetic errors (mispowerings, misalignments, and inhomogeneities) and orbit correction, is discussed. Computations using analytical and numerical methods are presented, and error tolerance specifications described.

INTRODUCTION

The CEBAF transport system is detailed elsewhere[1]. We now describe error analyses of this system. These were performed to analyze error sensitivities in the system and to develop tolerances for the design of beam transport system components. We remark that the CEBAF accelerator has aggressive emittance and energy spread goals of $\epsilon_{full} = 2 \times 10^{-9}$ m-rad and $\Delta E/E = 10^{-4}$. Investigation of error sensitivities and element specifications consistent with performance goals are therefore necessary. Earlier studies of this type have led to modifications of the transport system lattice; *e.g.*, implementation of "staircase" spreaders was made in response such analysis[2]. Subsequent studies, documented here and elsewhere[3], have led to further lattice development.

The investigation focusses on the recirculator, and observes certain restrictions. Only individual transport lines are considered (modularity is assumed). Nominal tunings alone are addressed. (Specialized tunings, such as spectrometer modes, are not considered.) As all 9 recirculation arcs are conceptually identical, simulation is performed for only a representative subset.

A similar analysis has been performed on the linacs[4], and is in progress for the complete machine[5].

SCOPE OF STUDY

Analytic methods provide order of magnitude estimates for beam line parameter sensitivity to single error sources, and serve to verify numerical results. Numerical simulation generates more precise results for isolated error dependences, and examines interactions of multiple errors. The following perturbations are addressed:

- transverse and longitudinal misalignments (including roll, yaw, and pitch)
- uncorrelated time independent excitation errors (such as DC mispowering or hysteresis) of major magnetic elements (dipoles, quadrupoles, and sextupoles)
- time dependent excitation errors, including uncorrelated mispowering of spreader/recombiner dipoles and all quadrupoles and sextupoles, as well as correlated mispowering of arc dipoles (which are in series), all quadrupoles, and sextupoles
- magnetic inhomogeneities in arc dipoles (including systematic quadrupole and multipole components and random quadrupole component) and quadrupoles (including systematic and random multipoles)

Model Of Magnetic Inhomogeneities

Arc dipoles are solid iron rectangular C magnets with a 1″ gap and 4.625″ pole width. The nominal peak field is 6 kG; 1, 2, and 3 m lengths are used. The pole width accommodates sagitta. The principle inhomogeneities are systematic quadrupole (from the asymmetry inherent in the C cross-section), random quadrupole (from assembly errors resulting in non-parallel pole placement), and systematic multipoles at the reference orbit (from exponential roll-off of the field near the pole edge).

We characterize the magnetic field profile in the arc dipoles as follows; $\kappa \equiv (\ln 10)/\delta$ and $A \equiv T/\cosh \kappa x_0$.

$$\frac{\Delta B(x)}{B} = \frac{A(1-\cosh \kappa x)}{(1-A)} + \left(\frac{B'_{sys} + B'_{ran}}{B}\right) x \qquad (1)$$

Here, x is the transverse displacement of the observation point relative to the straight-line geometric center of the pole (not the reference orbit), x_0 is half the "good field" of the magnet, δ is the distance over which the relative field error at the good field varies by a factor of ten, and T is the relative field error (the "tolerance") at the good field limit x_0. A value of 1 cm was used for δ in all studies; this is commensurate with the field rolloff for the 1 in. gap dipole[6]. B'_{sys} is the systematic, and B'_{ran} the random, quadrupole component. In simulations, (1) is translated to the design orbit, expanded in multipoles, and represented by multiple thin lenses distributed through the bend.

Recirculator quadrupoles are laminated iron magnets with full apertures of 1.125″ or 2.125″; 0.15 m and 0.3 m lengths are used. Nominal peak fields are under 4 kG at the pole. The principle inhomogeneities are systematic dodecapole and icosapole terms (from pole and end shapes), and random normal and skew multipoles (from construction errors). Using a multipole expansion $B(x) = (B\rho)\sum_{n=1}^{10} k_n x^n$, we employ systematic values for k_5 and k_9, and random values for k_2 through k_{10}, with random azimuthal phase. Variations in k_1 due to assembly errors

*Supported by D.O.E. contract #DE-AC05-84ER40150
†Now at SSCL

0-7803-0135-8/91$01.00 ©IEEE

are separately introduced as a random time-independent excitation error.

We employ a model in which assembly error generated random multipoles with $n \geq 2$ all contribute equal rms field errors at pole radius r_0. Denoting by a_s the relative rms field error from each multipole at the pole, rms multipole amplitudes will scale with excitation k_1 as follows.

$$\langle k_n \rangle_{rms} = \frac{a_s k_1}{r_0^{n-1}} \tag{2}$$

Equation (2) is evaluated for specified a_s, giving an rms value for the amplitude of every multipole in each magnet. An amplitude selected from a distribution with this rms width is then assigned to the quadrupole, using an azimuthal phase selected randomly from a uniform distribution on the interval $[0, 2\pi]$. In simulations, multipoles are represented by a thin lens embedded in the element.

ANALYTIC METHODS

Analytic studies address the effect of individual error sources in a specified beam line on lattice parameters at a downstream observation point (generally chosen to be the start of the next linac). Emphasis was placed on estimating transverse and longitudinal displacements, and transverse focal effects, due to the errors described above.

Steering Errors

An integral field error ΔBl deflects the beam through an angle $\Delta Bl/B\rho$, resulting in a downstream displacement. A set of N such random errors produces the following rms displacement, in either plane, at an observation point o[7].

$$\langle d \rangle = \sqrt{\frac{N}{2}\beta_o \overline{\beta}}\, \langle \frac{\Delta Bl}{B\rho} \rangle \tag{3}$$

Here, $\overline{\beta}$ is the mean beta function at the error sites; β_o is the value at o, and $\langle\ \rangle$ denotes an rms value. We use (3) to estimate the effect of missteering by quadrupole misalignments, dipole excitation errors, and power supply ripple in correction magnets and quads in which there are residual orbit errors.

Focussing Errors

Analogous relations give estimates of the impact of focussing errors. N random focussing perturbations characterized by rms focussing power $\langle P \rangle \equiv 1/\langle f \rangle$ (with $\langle f \rangle$ the rms effective focal length) generate deviations in lattice functions at a downstream point o[8]. Reasoning analogous to that giving (3) yields the following results for the rms deviations in lattice functions (in either plane) at o due to N perturbations with rms focussing power $\langle P \rangle$.

$$\begin{aligned} \langle \frac{\Delta\beta}{\beta_o} \rangle &= \sqrt{\frac{N}{2}}\, \langle P \rangle \overline{\beta} \\ \langle \Delta\alpha \rangle &= \sqrt{\frac{N}{2}\,(1+\alpha_o^2)}\, \langle P \rangle \overline{\beta} \\ \langle \Delta\psi \rangle &= \frac{1}{4\pi}\sqrt{\frac{N}{2}\,(3+\alpha_o^2)}\, \langle P \rangle \overline{\beta} \end{aligned} \tag{4}$$

Again, $\overline{\beta}$ is the average value at the error sites; α_o is the value at o. We use (4) to estimate the impact of focussing errors such as DC and AC excitation errors in quadrupoles and magnetic inhomogeneities in dipoles and quads.

NUMERICAL METHODS

Simulation allows for interaction of errors *via* the presence of multiple error sources, and for assessing the impact of a single error with great precision. Extensive modeling of error effects has been performed using DIMAD[9],[10]. As noted, all lines are conceptually identical so simulation is limited to 3 of the 9 lines. These were 445 MeV line (nominal tuning, which is the "typical" isochronous imaging achromat), the 3645 MeV line (also an imaging isochronous achromat, but with longer dipoles) and the 1645 MeV line (which is isochronous and achromatic but employs a nonimaging reinjection tuning) Modularity is assumed, so each line (from linac to linac) is treated independently.

All errors presented above are analyzed in conjunction. To manage the magnitude of the effort, errors were not varied independently; instead, a procedure aimed at setting design specifications was used. To establish the effect of a particular error and generate a tolerance, a subset of the above errors were chosen to have values consistent with earlier specifications. For a selected line, an error parameter of interest was then scanned over a wide range (typically from zero to a level giving large distortions in lattice parameters). This was done for several random error distributions (*viz.*, choices of "starting seed"). The dependence of relevant parameters, verses error level, was then recorded for each seed.

As an example, we present a scan of β_x dependence in the 445 MeV line on random errors in quadrupoles. Figure 1 illustrates the dependence, in ten randomly selected machines, of β_x at the reinjection point on a_s. Before generating Figure 1, tolerances for alignment and powering had been set, as had limits for systematic multipoles in the quads. Random selection of errors from distributions consistent with these specifications was made for each of the ten cases displayed (ten choices of "seed".) A value for β_x was then computed for ten values of a_s in each case. Figure 1 thus summarizes 100 DIMAD runs. Analysis of such results provides a tolerance for a_s. This specification is added to the list of parameters used during further study. This is the case in Figure 2, which illustrates, for ten randomly selected machines, a scan of β_x over the dipole good-field parameter x_0. Here, in addition to all errors employed in generating Figure 1, random multipoles in quadrupoles are added, with values specified by $a_s = 0.001$.

OBSERVED EFFECTS AND RESULTS; SPECIFICATIONS FOR TRANSPORT SYSTEM

The system shows no undue misalignment sensitivity; lattice parameters in the uncorrected machine depend linearly on rms misalignments up to about 0.6 mm. All parameters lie near design values after orbit correction. Modeling indicates a 200 μm alignment tolerance for all major elements is sufficient. Further analytic study indicates this applies to quadrupoles alone; 500 μm is sufficient for dipoles and sextupoles. Lattice parameter sensitivity to roll errors (especially in dipoles) leads to a stringent rms roll tolerance of 1 mrad. Although this is achieveable, reduction of roll sensitivity has been made by splitting the horizontal and vertical arc phase advances[11].

Study of power supply ripple effects indicate that care is needed in power supply specification. Such concerns lead, *e.g.*, to ganging of spreader power supplies. An earlier scheme of powering spreader dipoles independently generates tracking errors, causing centroid steering driven emittance dilution and path length wobble leading to momentum spread degradation. Analytic and numerical studies indicate that a 10^{-5} major dipole power supply stability, and a 10^{-4} quadrupole, sextupole, and correction dipole tolerance, assure the requisite beam stability to provide design phase space goals.

Analysis of systematic and random gradient errors in arc dipoles indicate these act as simple focussing perturbations, which may be compensated through trims of arc quadrupoles. Systematic nonlinear multipoles in dipoles are benign provided the beam resides within the good field of the magnet. Arc dipoles have therefore been designed with sufficient pole width to accommodate both the sagitta of the orbit and an additional "working aperture", over which the relative field error is below 10^{-3}. The good field is (sagitta+3.32 cm) horizontal × 2.0 cm vertical.

Systematic and random multipoles in quads generate orbit dependences in the optics and make the simulation of orbit correction more delicate by virtue of numerical sensitivity to nonlinearities. Unacceptable consequences of this error can be avoided by meeting the following conditions. First, the relative field error at the pole from any single multipole error source should be at or below the 0.1% level; secondly, rms residual orbit errors should be suppressed to the 1 – 2 mm level or below. Thirdly, beam emittances should be below the 10^{-7} m-rad level, and finally, momentum spreads or offsets should not exceed ±1/3%. Under these readily achieved conditions, machine parameters remain near their design values.

ACKNOWLEDGEMENTS

We are pleased to note extensive contributions by Dr. Roger Servranckx. We thank Dr. Leigh Harwood for useful discussions, in particular about magnetic inhomogeneities. Dr. Jörg Kewisch and Mr. Bruce Bowling have provided many useful interactions.

REFERENCES

[1] B. Bowling *et al.*, "The CEBAF Beam Transport System Lattice Design", these proceedings.

[2] D.R. Douglas *et al.*, "Optical Design of the CEBAF Beam Transport System", *Proc. 1989 I.E.E.E. Part. Accel. Conf.*, Chicago, Il., March, 1989, pp. 557-559.

[3] B. Bowling *et al.*, *op. cit.*

[4] R.C. York and J.Y. Tang, unpublished.

[5] B. Bowling *et al.*, CEBAF-TN-0168, Sept. 1989.

[6] L. Harwood, private communication.

[7] D.R. Douglas and R.C. York, "Perturbation Effects in the CEBAF Beam Transport System" *Proc. 1987 I.E.E.E. Part. Accel. Conf.*, Washington, D.C., Mar., 1987, pp. 1295-1297.

[8] D. Douglas, "Chromatic Correction in the CEBAF Transport System", these proceedings.

[9] R.V. Servranckx, *et al.*, "Users' Guide to the Program DIMAD", SLAC Report 285 UC-28 (A), May, 1985.

[10] D. Douglas *et al.*, CEBAF-TN-0141, Apr., 1989; CEBAF-TN-0175, Sept., 1989.

[11] See reference [1].

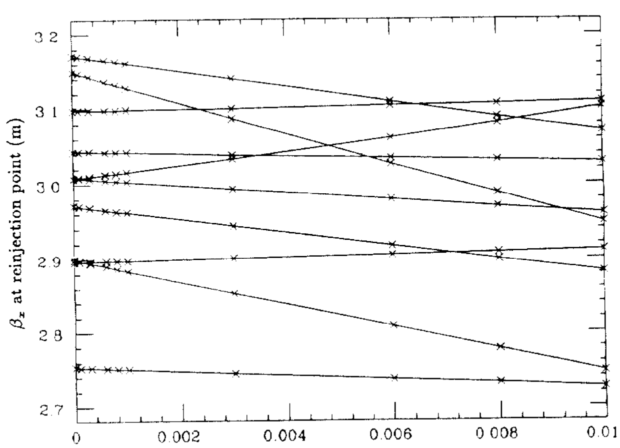

Figure 1. On-momentum β_x at end of in 445 MeV line *vs.* rms relative quadrupole field error a_s. Fixed effects also simulated include misalignments, orbit correction, DC excitation errors, and systematic multipoles in quadrupoles.

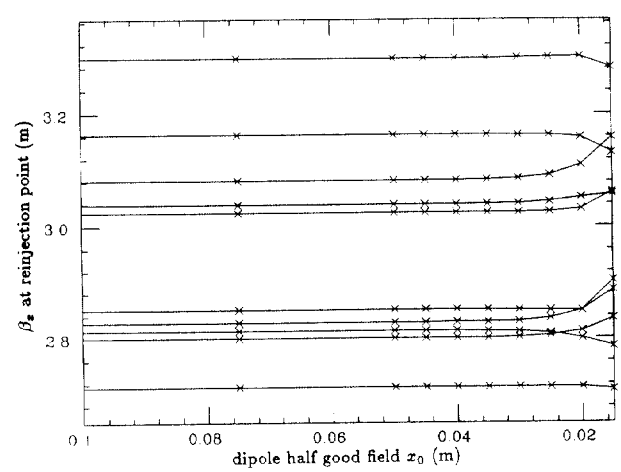

Figure 2. On-momentum β_x at end of in 445 MeV line *vs.* half good-field of dipole x_0. Fixed effects also simulated include misalignments, orbit correction, DC excitation errors, and systematic and random multipoles in quadrupoles.